Reaction Chemistry & Engineering

# Quantifying synergy for mixed end-scission and random-scission catalysts in polymer upcycling



| | |
|---|---|
| Journal: | *Reaction Chemistry & Engineering* |
| Manuscript ID | RE-ART-07-2023-000390.R1 |
| Article Type: | Paper |
| Date Submitted by the Author: | 04-Sep-2023 |





| | |
|---|---|
| Complete List of Authors: | Chen, Ziqiu; University of Illinois at Urbana-Champaign, Chemical and Biomolecular Engineering<br>Ejiogu, Emmanuel; University of Illinois at Urbana-Champaign, Chemical and Biomolecular Engineering<br>Peters, Baron; University of Illinois Urbana-Champaign, Chemical and Biomolecular Engineering |

# Quantifying synergy for mixed end-scission and random-scission catalysts in polymer upcycling

**Ziqiu Chen[1], Emmanuel Ejiogu[1], Baron Peters*[1, 2]**
[1] *Department of Chemical and Biomolecular Engineering, University of Illinois at Urbana-Champaign, Urbana, IL 61801, USA.*
[2] *Department of Chemistry, University of Illinois at Urbana-Champaign, Urbana, IL 61801, USA*
** Corresponding author, Email: baronp@illinois.edu*

**Abstract**: The environmental consequences of plastic waste are driving research into many chemical and catalytic recycling strategies. The isomerizing ethenolysis strategy for polyethylene upcycling combines three catalysts to affect two different actions: non-processive scission at chain ends, and scission at random interior points. We show that population balance equations (PBEs) based on the local density approximation (LDA) accurately describe the end-scission chemistry. We further show that the model can be simplified to a first-order PBE when started from a realistic molecular weight distribution. The simplification enables formulation and solution of a model that includes both end-scission and random-scission modalities. The mixture of catalysts (in theory) can exhibit a quantitative synergy, e.g., with the total number of cuts for the catalyst mixture exceeding that for the sum of its separate component catalyst actions. We develop equations to predict and optimize the synergistic acceleration.

Keywords: polymer upcycling, ethenolysis, end-scission, random-scission, tandem catalysis

## Introduction

Over 300 million tons of plastics are produced every year, yet less than 10% is recycled.[1-3] Most is incinerated, landfilled, or discarded into the natural environment. Chemical recycling processes, especially with catalysts to guide selectivity, have the potential to create high value chemicals from plastic waste.[4-17] Different catalysts for polymer upcycling operate in different ways: end scission or random scission, heterogeneous or homogeneous, processive or non-processive, etc. Processes that use a mixture of catalysts may even exploit synergies between different catalyst modalities.[18-26]

Current research in catalytic polymer upcycling is mainly empirical,[27-40] with only a small fraction of studies attempting theoretical analysis of the underlying reaction mechanisms and reaction progress.[41-49] Based on an extrapolation from other branches of catalysis,[50-62] theoretical models and calculations will likely have a major impact on polymer upcycling, from understanding the chemistry, to developing new catalysts, to industrial process design. However, polymer upcycling presents several unique challenges for theory and computation.[49] The polymer mixture typically contains chains with millions of different molecular weights having different degrees and types of functionalization.

Population balance equations (PBEs) are analogous to the more familiar species balance equations (often called rate equations), but PBEs describe a continuous distribution rather than a short discrete list of reagents.[63, 64] Several recent studies have used PBEs to model the evolution of molecular weight distributions (MWDs) and generation of products during catalytic polymer upcycling processes.[45, 49]

This study is motivated by recent experiments that combine polyethylene with excess ethylene and three catalysts: a double-bond isomerization catalyst, a metathesis catalyst, and a dehydrogenation catalyst.[18, 20] The first two catalysts cooperate to affect end-scission via a complex isomerizing ethenolysis reaction. In brief, this reaction uses ethylene to excise $CH_2$ units from the ends of vinyl terminated polyethylene chains, leaving a propylene product and a shortened chain. Prior to the experimental works, Guironnet and Peters described the mechanism and modeled the double-bond isomerization and metathesis kinetics in isomerizing ethenolysis.[45] In the subsequent experiments, the third dehydrogenation catalyst

was added to create double bonds at random interior locations.[18, 20] The double bonds allow the chain to also be cut at random locations upon metathesis with ethylene. The random-scission events should result in more chains with double bonds at both ends, and thereby accelerate the isomerizing ethenolysis reaction.

At present, the isomerizing ethenolysis and dehydrogenation catalysts do not work together as intended.[18, 20] However, end scission and random scission are common catalysis motifs, and nature has already combined them. For example, fungi use a cocktail of cellulases to depolymerize cellulose, with random scission by the endocellulases creating new chain ends which are then attacked by exocellulases. In the cellulase literature, the synergy between these enzymes was anticipated in many studies[65-68] and several works modeled the enzymatic reactions with discrete rate equations and population balance equations.[69-72] One population balance study demonstrated the synergy between end-scission and random-scission enzymes, although no recipe for the synergy calculation was provided.[72]

In this work, we revisit the second-order PBE developed by Guironnet and Peters.[45] Using numerical solutions to the complete set of double-bond isomerization and metathesis rate equations as a standard, we show that the full PBE, as well as a simplified first-order version of the PBE, both yield accurate solutions for realistic initial MWDs. Then we combine the first-order model for end scission with birth and death terms in the PBE for random scission. We provide a new analytic solution to the combined PBE for end scission and random scission and predict the synergistic acceleration due to the combination of random-scission and end-scission catalysts. Finally, we discuss how these results might be used to optimize the catalyst mixture to achieve the maximum acceleration.

## Revisiting the isomerizing ethenolysis model

Guironnet and Peters presented a kinetic model for polymer upcycling with tandem double bond isomerization and olefin metathesis catalysts.[45] They started with rate equations for all olefin species, and used pseudo-steady state approximations (PSSAs) and local density approximations (LDAs), to convert the massive ODE system into one Fokker-Planck-type equation:

$$\frac{\partial \rho}{\partial t} + \dot{n}\frac{\partial \rho}{\partial n} = D_n \frac{\partial^2 \rho}{\partial n^2} \tag{2}$$

with

$$\frac{\dot{n}}{k_D} = -\frac{2}{1+\sqrt{(4+\kappa)/\kappa}} \tag{3}$$

and

$$\frac{D_n}{k_D} = \frac{\sqrt{(4+\kappa)/\kappa}}{1+\sqrt{(4+\kappa)/\kappa}} \tag{4}$$

Here $\kappa$ is the ratio of the metathesis rate over the isomerization rate and $k_D$ is the isomerization rate, i.e., the frequency at which a double bond changes position on the olefin chain. In equations (3)-(4), $\dot{n}$ represents the chain shortening rate, and $D_n$ represents the rate at which dispersity grows in the polymer distribution. Equation (2) is different from typical PBEs because it does not invoke the coefficients as adjustable phenomenological parameters. Rather, the coefficients are expressions derived from details of the underlying mechanism. Detailed derivations of (2)-(4) as well as the starting rate equations, can be found in Guironnet and Peters.

There are several methods for modeling end-scission depolymerizations, including numerical methods and analytic solutions[44] for discrete rate equations[73, 74] and for PBEs.[75-77] Guironnet and Peters compared numerical solutions for the complete set of double-bond isomerization and ethene metathesis rate equations to analytic solutions from the simplified PBE in equations (2)–(4).

Guironnet and Peters focused on a sharp monodisperse initial MWD. They found that the PBE yielded highly accurate solutions for $\kappa > 1$, but less accurate solutions for $\kappa < 1$. In **Figure 1** we similarly compare numerical solutions to (analytic) PBE solutions, but we start with a more realistic polydisperse initial MWD. Note that the

calculated MWDs from equation (2) do not include the propylene products.

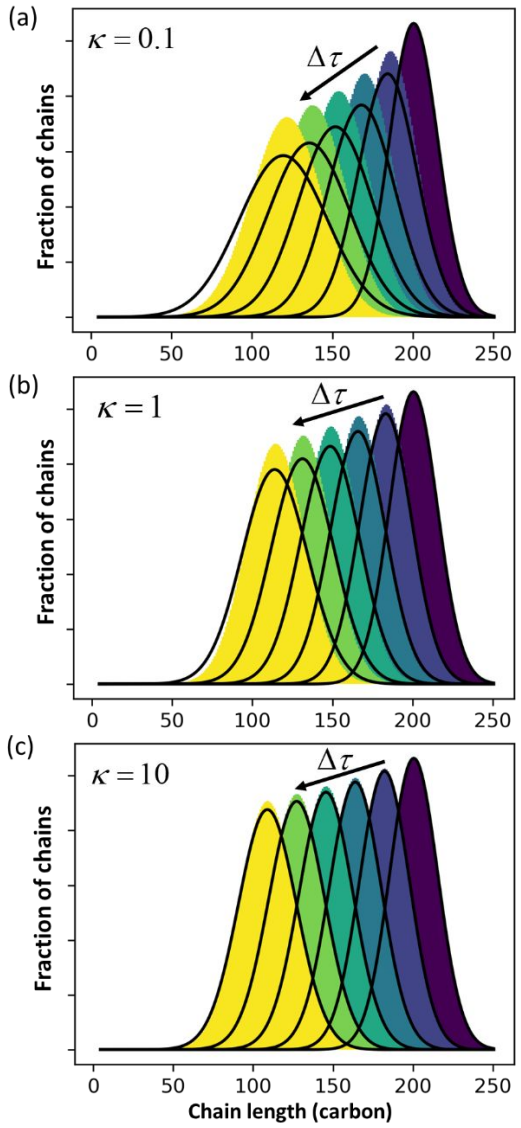


**Figure 1. Comparison between exact solution from rate equations and solutions of equation (1) for (a) $\kappa = 0.1$; (b) $\kappa = 1$ (c) $\kappa = 10$.**

The accuracy of equation (1) decreases when olefin metathesis is slower than double bond isomerization, i.e., when $\kappa < 1$. In the derivation of equation (1), the LDA ignores gradient [$\partial\rho/\partial n$] terms when applying the PSSA to the distribution of double bond positions. If we include gradient terms when applying the PSSA equations, the resulting PBE becomes nonlinear and no longer admits analytical solutions.

An analysis of error contributions suggests that the average "drift velocity" term, i.e., that containing $\dot{n}$, contributes negligible errors. The inaccuracies for $\kappa < 1$ are entirely due to an exaggerated increase in polydispersity, i.e., from an overestimation of $D_n$.

We can estimate the importance of polydispersity errors as follows. The predicted variance in the MWD over time can be calculated by the mean square displacement: $\Delta n^2(t) = \Delta n^2(0) + 2D_n t$,[78, 79] where $\Delta n^2(t)$ is the variance of the MWD at time $t$. The time required to consume chains of an average initial length $M_n(0)$ is:

$$t_{\max} = \frac{M_n(0)}{\dot{n}} \qquad (5)$$

Therefore, we have $\Delta n^2_{\max} = \Delta n^2(0) + 2D_n M_n(0)/\dot{n}$ where both $D_n$ and $\dot{n}$ can be written in terms of $\kappa$ using equations (2) and (3). The result gives an estimate for the variance in the MWD as the reaction approaches completion:

$$\Delta n^2_{\max} = \Delta n^2(0) + \sqrt{4+\kappa/\kappa}\, M_n(0) \qquad (6)$$

When the added variance from the second derivative term $[((4+\kappa)/\kappa)^{1/2} M_n(0)]$ is smaller than the initial variance $[\Delta n^2(0)]$, it makes little difference whether the second derivative term is included or neglected. That is, for the ratio $[\Delta n^2_{\max}/\Delta n^2(0)]$, when it is close to 1, the dispersion term does not affect the results, and when it is much larger than 1, then the dispersion term becomes very important to the PBE. Indeed, for realistic initial MWDs the second derivative term may be omitted entirely. We illustrate this in **Table 1**:

| | parameters | $\Delta n^2_{\max}/\Delta n^2(0)$ | Dispersion from 2°-term |
|---|---|---|---|
| **Fig 1a** | $M_n(0) = 200$<br>$\Delta n(0) = 15$<br>$\kappa = 0.1$ | 6.78 | Very important. Small errors matter. |

| | | | |
|---|---|---|---|
| **Fig 1c** | $M_n(0) = 200$<br>$\Delta n(0) = 15$<br>$\kappa = 10$ | 2.04 | Moderately important. OK to make small errors. |
| Conk et al. | $M_n(0) = 3276$<br>$\Delta n(0) = 2000$<br>$\kappa = 0.1$* | 1.00 | Unimportant. Can entirely omit 2°-term |

**Table 1. Inaccuracies emerging from the second order (2°) term in the LDA-derived PDE. The 2°-term is important for small initial molecular weights, but inconsequential for realistic PE materials with broad MWDs.**

Note that the MWD can be scaled with the mass of $CH_2$ to recover the distribution of chain concentrations, and that all calculations in **Table 1** are performed in the number of carbons instead of Daltons for simplicity. The analysis in **Table 1** suggests that, for initial MWDs like those from commercial plastics, the second-order term in equation (2) can be entirely neglected.

In **Figure 2** we let $\rho_0(n)$ be the initial MWD from the experiments of Conk *et. al.* on isomerizing ethenolysis of polyethylene.[20] **Figure 2a** solves the equation using the LDA-derived PBE as written in equation (2). **Figure 2b** presents the solution for the same initial conditions and same PBE, but with the second-order term omitted. In this case, the PBE becomes:

$$\frac{\partial \rho}{\partial t} + \kappa \frac{\partial \rho}{\partial n} = 0 \qquad (7)$$

and the solution (e.g., from the method of characteristics) is:

$$\rho(n,t) = \rho_0(n - \kappa t) \qquad (8)$$

Note that the mass is not conserved because the propylene products are not included in $\rho(n,t)$.

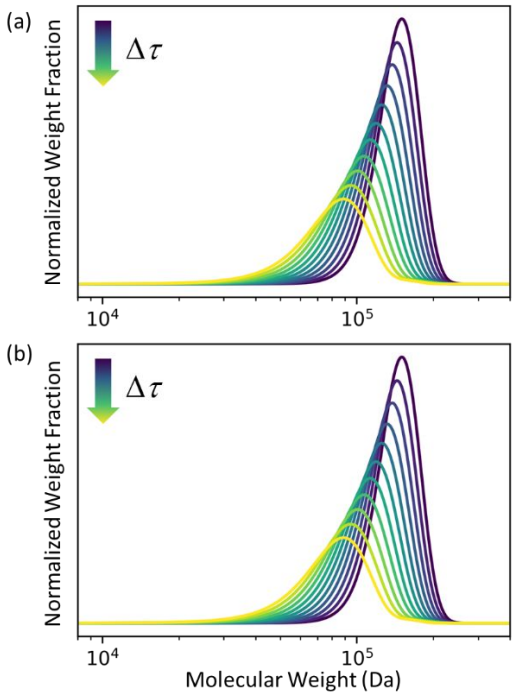


**Figure 2. (a) Predicted MWD evolving with time according to equation (1) with $\kappa = 1$. (b) Predicted MWD evolving with time from equation (6) with $\kappa = 1$.**

There is no apparent difference between **Figure 2a** and **Figure 2b**, which confirms our prediction that the first order term in the LDA-derived PBE is sufficient for predicting the MWD evolution with realistic initial MWDs. We emphasize that this conclusion should be generally applicable to any end-scission upcycling mechanism, and not specific to isomerizing ethenolysis.

### Tandem end scission and random scission

In this section, we build a model for tandem end-scission and random-scission catalysts. End scission results in a new chain of length that is slightly smaller than that of the parent chain. Because the changes in molecular weight from end scission are small, the result is a gradual drift-like term in the PBE. In contrast, random scission results in new chains of completely different lengths from the parent chain. Thus, random scission must be modeled using birth and death

terms.[80] The combined result of both end scission and random scission is the PBE:

$$\frac{\partial \rho}{\partial t} + \frac{\partial (\dot{n}\rho)}{\partial n} = -k_c n \rho(n,t) + 2k_c \int_n^\infty \rho(n',t)\, dn' \quad (9)$$

Here $\dot{n}$ is the rate of chain shortening on the end as in (3), and thus will be a negative value. And $k_c$ is the rate of random scission per carbon-carbon bond. The birth and death terms on the right-hand side of equation (9) are explained in the references.[49, 80] The combined equation was also obtained in work on end-scission and random-scission by cellulases.[72]

To enable a systematic analysis of synergy, we pursue a nondimensionalization that balances end-scission and random-scission contributions. First, we nondimensionalize chain length using the initial mean chain length of the polymer, that is:

$$N \equiv \frac{n}{M_n(0)} \quad (10)$$

We refer to $N$ as the relative chain length throughout the remainder of the manuscript. Correspondingly, we have:

$$\rho_N = \rho \frac{dn}{dN} = \rho M_n(0) \quad (11)$$

Then, we define the nondimensional time as the real time multiplied by the sum of two contributions: the frequency of new chain creation by a random scission and the frequency of entire chain digestion via end scission:

$$\tau \equiv \left( M_n(0) k_c + \frac{\dot{n}}{M_n(0)} \right) t \quad (12)$$

Now, we define a new term $\alpha$:

$$\alpha \equiv \frac{k_c M_n(0)}{k_c M_n(0) + \dot{n} M_n(0)} \quad (13)$$

which can be interpreted as the fraction of chains at the initial average length that get cut at a random location before complete digestion from the end.

With these definitions, the nondimensional form of equation (9) becomes:

$$\frac{\partial \rho_N}{\partial \tau} + \frac{\partial}{\partial N}\left[ (1-\alpha)\rho_N \right] = -\alpha N \rho_N + 2\alpha \int_N^\infty \rho_N(N',\tau)\, dN' \quad (14)$$

We solved equation (14) numerically over nondimensional time $\tau$ by first converting the equations into a series of ODEs. Then, using a normal distribution as the initial condition, we use Scipy v1.4.1[81] to solve the initial value problem. The backward differentiation formula (BDF) is chosen as the ODE solver for stability and convergence. The solutions are shown in **Figures 3a** and **3b** for the limiting cases where there is only random scission ($\dot{n}$ = 0 and $\alpha$ = 1) and only end scission ($k_c$ = 0 and $\alpha$ = 0), respectively. **Figure 3c** shows the solutions for a case where both catalysts work together at ratio $\alpha$ = 0.95. The effects of random cuts are most pronounced when nearly all chains get randomly cut before they are consumed by end-scission.

We also developed an analytical solution for equation (14) using the strategy from Ziff and McGrady,[82]

$$\begin{aligned} \rho(N,\tau) &= \zeta(N,\tau)\rho(N+(1-\alpha)\tau,0) \\ &+ \zeta(N,\tau) 2\alpha\tau \int_N^\infty \rho(z+(1-\alpha)\tau,0)\, dz \\ &+ \zeta(N,\tau)(\alpha\tau)^2 \int_N^\infty \rho(z+(1-\alpha)\tau,0)(z-N)\, dz \end{aligned} \quad (15)$$

where

$$\zeta(N,\tau) = \exp\left[ -\alpha\tau \left( N - (1-\alpha)\frac{\tau}{2} \right) \right] \quad (16)$$

To check the derivation, we confirmed that the analytic solution matches the numerical solutions. See SI for detailed derivations and results.

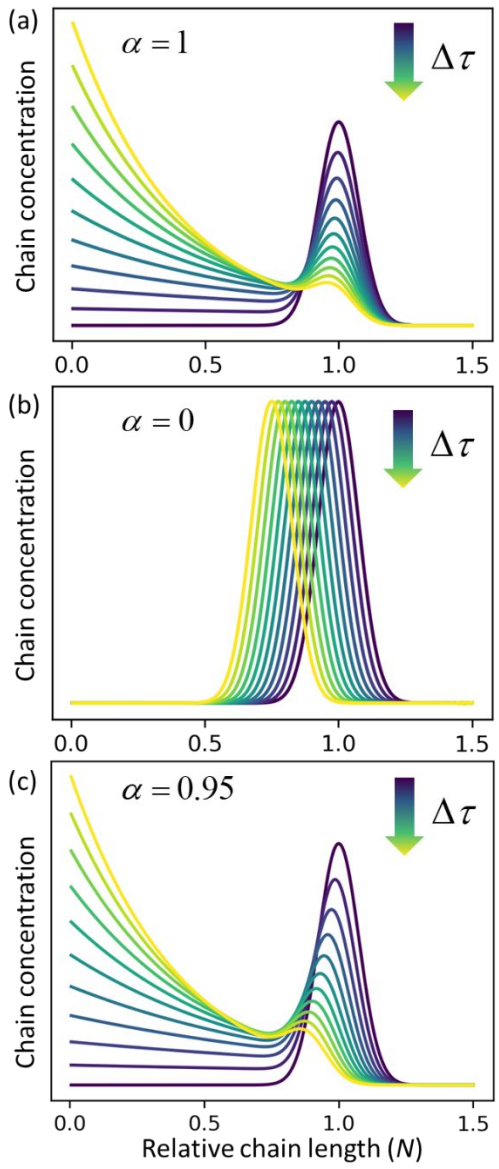


**Figure 3. Time evolution of the relative chain length distribution for three cases. (a) Only random-scission, i.e., $\alpha = 1$; (b) Only end-scission, i.e., $\alpha = 0$; (c) Both end- and random-scission with $\alpha = 0.95$. All three calculations begin from a normal distribution in relative chain length $N$ with a mean of 1.0 and standard deviation of 0.075.**

The solutions in **Figure 3** resemble those from analysis of combined end-scission and random-scission of cellulose by cellulase enzymes. In the following section, we exploit the non-dimensionalization to provide an expression that quantifies synergy of the end-scission and random-scission catalysts.

### Quantifying synergy with cutting rates

When both end-scission and random-scission rates are nonzero, the number of chain ends will increase with time due to random scission. If excess end-scission catalyst is available, the overall rate of conversion should increase with time. To quantify the number of cuts, we first decompose $\dot{n}$ as:

$$\dot{n} = k_E \Delta n \tag{17}$$

where $k_E$ is the number of end-scission events per time per chain, and $\Delta n$ is the segment size per end scission. For isomerizing ethenolysis, $\Delta n = 1$. The rate of end scission is:

$$\begin{aligned} r_E &= \int_0^\infty k_E \rho(n,t)\, dn \\ &= \frac{M_n(0)}{\Delta n} \int_0^\infty \frac{\dot{n}}{M_n(0)} \rho_N(N,\tau) dN \end{aligned} \tag{18}$$

Similarly, the rate of random scission is:

$$\begin{aligned} r_R &= \int_0^\infty k_c \rho(n,t)\, n dn \\ &= \int_0^\infty k_c M_n(0)\, N \rho_N(N,\tau)\, dN \end{aligned} \tag{19}$$

$r_E$ and $r_R$ can be normalized by $k_c M_n(0) + \dot{n}/M_n(0)$ and then written in terms of the dimensionless $\alpha$. With these simplifications, the total (normalized) scission rate, with both random- and end-scission events occurring at the same time, is:

$$\begin{aligned} &\frac{r_E + r_R}{k_c M_n(0) + \dot{n}/M_n(0)} \\ &= \frac{M_n(0)}{\Delta n}(1-\alpha) \int_0^\infty \rho_N(N,\tau) dN \\ &\quad + \alpha \int_0^\infty N \rho_N(N,\tau) dN \end{aligned} \tag{20}$$

Now to quantify the synergistic acceleration of the mixed catalyst system, we compare the rate in equation (17) to that for limiting cases with end scission or random scission occurring separately.

For a system with only end scission, at the same physical time $t$, define the nondimensional time $\tau_0$ as:

$$\tau_0 = \frac{k_c M_n(0)}{M_n(0)} t = (1-\alpha)\tau \tag{21}$$

Then we solve

$$\frac{\partial \rho_N^0}{\partial \tau_0} + \frac{\partial \rho_N^0}{\partial N} = 0 \tag{22}$$

to predict the time evolution of the molecular weight distribution $\rho^0_N(N, \tau_0)$ with only end scission. Note that we are not actually changing the rate parameters for end or random scission relative to those in equation (17). Rather, we are solving for the molecular weight evolution and scission rates *as though the two scission mechanisms are occurring separately*.

For end scission alone, the normalized scission rate is:

$$\frac{r_E^0}{k_c M_n(0) + k_c M_n(0)} = \frac{M_n(0)}{\Delta n}(1-\alpha)\int_0^\infty \rho_N^0\left(N,(1-\alpha)\tau\right)dN \tag{23}$$

For the system with only random scission, we define $\tau_1$ as:

$$\tau_1 = k_c M_n(0) t = \alpha\tau \tag{24}$$

Then we solve

$$\frac{\partial \rho_N^1}{\partial \tau_1} = -N\rho_N^1 + 2\int_0^\infty \rho_N^1 N dN \tag{25}$$

to predict the time evolution of the molecular weight distribution $\rho^1_N(N, \tau_1)$ with only random scission. Now the normalized rate with random scission alone is

$$\frac{r_R^1}{k_c M_n(0) + k_c M_n(0)} = \alpha\int_0^\infty N\rho_N^1\left(N,\alpha\tau\right)dN \tag{26}$$

To compare the rate with both catalysts operating simultaneously (equation 17) to the rates of their separate actions, we add the rates in equations (22) and (23). In other words, we can directly compare $r_E + r_R$ to $r^0_E + r^1_R$.

We define the synergistic acceleration as $\eta(\alpha, \tau) = (r_E + r_R)/(r^0_E + r^1_R)$. From equations (20), (23),and (26), the synergistic acceleration is a function of $\alpha$, $\tau$, and $M_n(0)/\Delta n$.

$$\eta\left(\alpha,\tau,M_n(0)/\Delta n\right) = \frac{\frac{M_n(0)}{\Delta n}(1-\alpha)\int_0^\infty \rho_N(N,\tau)dN + \alpha\int_0^\infty N\rho_N(N,\tau)dN}{\frac{M_n(0)}{\Delta n}(1-\alpha)\int_0^\infty \rho_N^0\left(N,(1-\alpha)\tau\right)dN + \alpha\int_0^\infty N\rho_N^1(N,\alpha\tau)dN} \tag{27}$$

When $\alpha$ = 0.0 or $\alpha$ = 1.0, the synergistic acceleration factor $\eta \rightarrow 1.0$. For all intermediate values it initially climbs to a value larger than unity. At long times, as the reaction completes, the acceleration factor drops below unity because the mixed catalyst system more rapidly reaches a point where all chains have been cut to propylene and butadiene.

Note that derivations from equation (17) to equation (27) assume cutting rates are only determined by the number of chains and C-C bonds with no limitation on the catalyst amount. Situations where the rate of end scission becomes limited by the availability of catalyst will require additional analysis.

**Figure 4** plots $\eta$ as a function of dimensionless time and a for three different values of the initial chain length parameter $M_n(0)/\Delta n$. The first initial chain length parameter, $M_n(0)/\Delta n$ = 40, corresponds approximately to the lengths of chains at the onset of isomerizing ethenolysis in the work of Conk et al.[20] The chains are unusually short because they are randomly dehydrogenated before the isomerizing ethenolysis step. Therefore, the chains of Conk et al. undergo metathesis with ethane to give short chains very early in the isomerizing ethenolysis process.

Results for the other initial chain length parameters in **Figure 4**, $M_n(0)/\Delta n$ = 200 and $M_n(0)/\Delta n$ = 1000, show that the synergistic

acceleration becomes a relatively weak function of chain length for long chains.

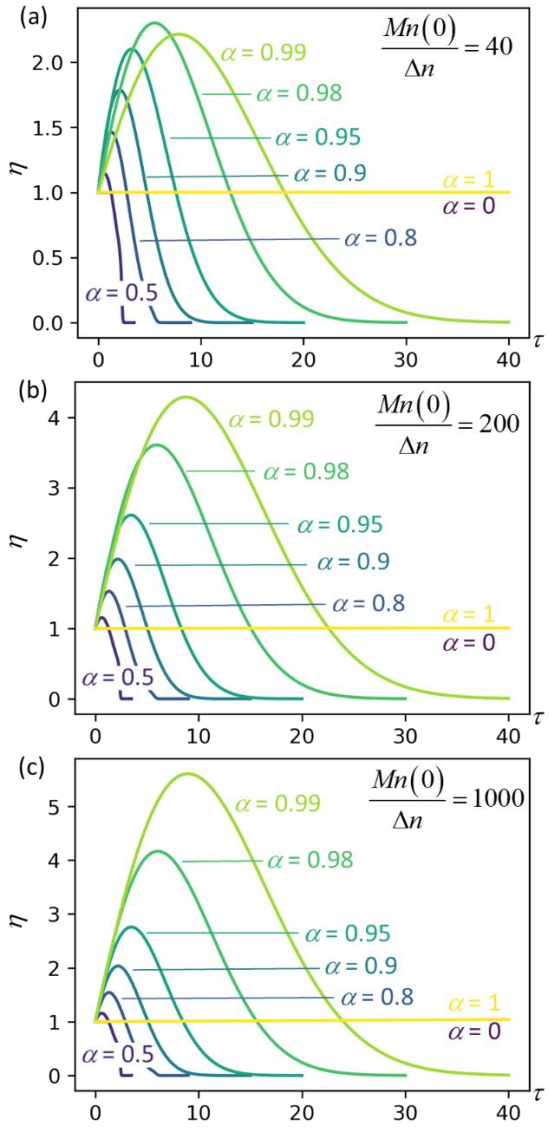


**Figure 4. Synergistic acceleration $\eta$ vs. dimensionless time at different $\alpha$ values with (a) $M_n(0)/\Delta n$ = 40; (b) $M_n(0)/\Delta n$ = 200; (c) $M_n(0)/\Delta n$ = 1000.**

We can see that all mixtures of end-scission and random-scission catalysts initially accelerate beyond the rate of the limiting cases ($\alpha = 0$ and $\alpha = 1$). $\eta$ first increases due to the newly generated chain ends from random scissions, and all the new chains are longer than the minimal cutting length. Then, as these chains reach the minimum length, $\eta$ starts to decrease, ultimately dropping to 0, which indicates the complete consumption of chains.

The results in **Figure 4** allow us to design the depolymerization process by varying $\alpha$ to maximize the cutting rate. Interestingly, the $\alpha$ value that maximizes the synergistic acceleration seems to be related to $M_n(0)/\Delta n$. For $M_n(0)/\Delta n$ = 40, the maximum synergy occurs for $\alpha$ = 0.98. For $M_n(0)/\Delta n$ = 200, the maximum synergy occurs for $\alpha$ = 0.995, as shown in the Supporting Information. For $M_n(0)/\Delta n$ = 1000, the maximum synergy occurs for $\alpha$ =0.999, as shown in the Supporting Information. In each case, the value of $\alpha$ that maximizes the synergy is approximately $\alpha = 1 - \Delta n/M_n(0)$. This design rule should be regarded as a conjecture, because as yet we cannot say whether it remains valid for all values of $M_n(0)/\Delta n$ nor provide a justification for its validity.

## Conclusion

For realistic initial molecular weight distributions (MWDs), this paper shows that a previous kinetic model for isomerizing ethenolysis by Guironnet and Peters can be dramatically simplified to the form of a first-order population balance equation (PBE). Motivated by recent experiments, which demonstrated the isomerizing ethenolysis chemistry and also explored the effects of an additional dehydrogenation catalyst, we extended the kinetic model to cases with mixed end-scission and random-scission catalysts.

A dimensionless parameter $\alpha$ that emerges from the model quantifies the relative rates of end scission and random scission. We provided an analytic solution to the combined end-scission and random-scission equation for any $\alpha$. We compare results from the two limiting cases of random-scission and end-scission to intermediate cases where both catalysts are working together. We show that, given sufficient end-scission catalyst, random scission causes a proliferation of new chain ends and thereby accelerates the overall depolymerization progress.

We developed a mathematical expression for the synergistic acceleration factor ($\eta$), i.e., the rate relative to the combined rate from the two independently occurring processes. $\eta$ depends on the initial average molecular weight, on the reaction time, and on the value of $\alpha$, i.e. the fraction of chains at the initial average length that get cut at a random location before they are completely digested from the chain ends. As time advances, $\eta$ begins at 1.0 (no acceleration), and gradually climbs to a maximum value that depends on $\alpha$ and the initial molecular weight. The results should be useful in understanding and optimizing the mixture of catalysts to achieve the maximum acceleration. Specifically, our analysis suggests that the value of $\alpha$ (and accordingly the catalyst mixture) that maximizes the synergy is approximately $\alpha = 1 - \Delta n/M_n(0)$.

## Author contributions

ZC was responsible for writing - original draft and editing, methodology, computational work, and data analysis. EE developed the analytical solution of PBE. BP was responsible for conceptualization, funding acquisition, project administration, supervision, and writing – review and editing.

## Conflicts of interest

The authors declare no conflict of interest.

## Acknowledgements

We thank members of the iCOUP team, Charles Sing, and Damien Guironnet for helpful discussions. This work was supported by the Institute for Cooperative Upcycling of Plastics (iCOUP), an Energy Frontier Research Center funded by the U.S. Department of Energy (DOE), Office of Basic Energy Sciences, Division of Chemical Sciences, Geosciences, and Biosciences, via subcontract from Ames National Laboratory. Ames National Laboratory is operated for the DOE by Iowa State University under Contract No. DE-AC02-07CH11358.

## References

1. Geyer, R.; Jambeck, J. R.; Law, K. L., Production, use, and fate of all plastics ever made. *Sci. Adv.* **2017,** *3*, e1700782.
2. Liang, Y.; Tan, Q.; Song, Q.; Li, J., An analysis of the plastic waste trade and management in Asia. *Waste Manage.* **2021,** *119*, 242-253.
3. Barnes, D. K.; Galgani, F.; Thompson, R. C.; Barlaz, M., Accumulation and fragmentation of plastic debris in global environments. *Philos. Trans. R. Soc. Lond., B, Biol. Sci.* **2009,** *364*, 1985-98.
4. Kosloski-Oh, S. C.; Wood, Z. A.; Manjarrez, Y.; de Los Rios, J. P.; Fieser, M. E., Catalytic methods for chemical recycling or upcycling of commercial polymers. *Mater. Horiz.* **2021,** *8*, 1084-1129.
5. Chen, H.; Wan, K.; Zhang, Y.; Wang, Y., Waste to Wealth: Chemical Recycling and Chemical Upcycling of Waste Plastics for a Great Future. *ChemSusChem* **2021,** *14*, 4123-4136.
6. Stadler, B. M.; de Vries, J. G., Chemical upcycling of polymers. *Philos. Trans. Royal Soc. A* **2021,** *379*, 20200341.
7. Jehanno, C.; Alty, J. W.; Roosen, M.; De Meester, S.; Dove, A. P.; Chen, E. Y.; Leibfarth, F. A.; Sardon, H., Critical advances and future opportunities in upcycling commodity polymers. *Nature* **2022,** *603*, 803-814.
8. Zhao, X.; Korey, M.; Li, K.; Copenhaver, K.; Tekinalp, H.; Celik, S.; Kalaitzidou, K.; Ruan, R.; Ragauskas, A. J.; Ozcan, S., Plastic waste upcycling toward a circular economy. *Chem. Eng. J.* **2022,** *428*.
9. Korley, L. T. J.; Epps, T. H., 3rd; Helms, B. A.; Ryan, A. J., Toward polymer upcycling-adding value and tackling circularity. *Science* **2021,** *373*, 66-69.
10. Li, X.; Wang, J.; Zhang, T.; Yang, S.; Sun, M.; Qian, X.; Wang, T.; Zhao, Y., Sustainable catalytic strategies for the transformation of plastic wastes into valued products. *Chem. Eng. Sci.* **2023,** *276*.
11. Hinton, Z. R.; Talley, M. R.; Kots, P. A.; Le, A. V.; Zhang, T.; Mackay, M. E.; Kunjapur, A. M.; Bai, P.; Vlachos, D. G.; Watson, M. P.*, et al.*,

Innovations Toward the Valorization of Plastics Waste. *Annu. Rev. Mater. Sci.* **2022,** *52*, 249-280.
12. Zhang, M.-Q.; Wang, M.; Sun, B.; Hu, C.; Xiao, D.; Ma, D., Catalytic strategies for upvaluing plastic wastes. *Chem* **2022,** *8*, 2912-2923.
13. Bidange, J.; Fischmeister, C.; Bruneau, C., Ethenolysis: A Green Catalytic Tool to Cleave Carbon-Carbon Double Bonds. *Chemistry* **2016,** *22*, 12226-44.
14. Faust, K.; Denifl, P.; Hapke, M., Recent Advances in Catalytic Chemical Recycling of Polyolefins. *Chemcatchem* **2023,** *15*.
15. Wei, J.; Liu, J.; Zeng, W.; Dong, Z.; Song, J.; Liu, S.; Liu, G., Catalytic hydroconversion processes for upcycling plastic waste to fuels and chemicals. *Catal. Sci. Technol.* **2023,** *13*, 1258-1280.
16. Tan, T.; Wang, W.; Zhang, K.; Zhan, Z.; Deng, W.; Zhang, Q.; Wang, Y., Upcycling Plastic Wastes into Value-Added Products by Heterogeneous Catalysis. *ChemSusChem* **2022,** *15*, e202200522.
17. Kots, P. A.; Vance, B. C.; Vlachos, D. G., Polyolefin plastic waste hydroconversion to fuels, lubricants, and waxes: a comparative study. *React. Chem. Eng.* **2022,** *7*, 41-54.
18. Wang, N. M.; Strong, G.; DaSilva, V.; Gao, L.; Huacuja, R.; Konstantinov, I. A.; Rosen, M. S.; Nett, A. J.; Ewart, S.; Geyer, R.*, et al.*, Chemical Recycling of Polyethylene by Tandem Catalytic Conversion to Propylene. *J. Am. Chem. Soc.* **2022,** *144*, 18526-18531.
19. Zhang, F.; Zeng, M.; Yappert, R. D.; Sun, J.; Lee, Y.-H.; LaPointe, A. M.; Peters, B.; Abu-Omar, M. M.; Scott, S. L., Polyethylene upcycling to long-chain alkylaromatics by tandem hydrogenolysis/aromatization. *Science* **2020,** *370*, 437-441.
20. Conk, R. J.; Hanna, S.; Shi, J. X.; Yang, J.; Ciccia, N. R.; Qi, L.; Bloomer, B. J.; Heuvel, S.; Wills, T.; Su, J.*, et al.*, Catalytic deconstruction of waste polyethylene with ethylene to form propylene. *Science* **2022,** *377*, 1561-1566.
21. Ahuja, R.; Kundu, S.; Goldman, A. S.; Brookhart, M.; Vicente, B. C.; Scott, S. L., Catalytic ring expansion, contraction, and metathesis-polymerization of cycloalkanes. *ChemComm* **2008,** 253-5.
22. Tennakoon, A.; Wu, X.; Paterson, A. L.; Patnaik, S.; Pei, Y. C.; LaPointe, A. M.; Ammal, S. C.; Hackler, R. A.; Heyden, A.; Slowing, I. I.*, et al.*, Catalytic upcycling of high-density polyethylene via a processive mechanism. *Nat. Catal.* **2020,** *3*, 893-901.
23. Achilias, D. S.; Roupakias, C.; Megalokonomos, P.; Lappas, A. A.; Antonakou, E. V., Chemical recycling of plastic wastes made from polyethylene (LDPE and HDPE) and polypropylene (PP). *J. Hazard. Mater.* **2007,** *149*, 536-42.
24. Zhou, H.; Wang, Y.; Ren, Y.; Li, Z.; Kong, X.; Shao, M.; Duan, H., Plastic Waste Valorization by Leveraging Multidisciplinary Catalytic Technologies. *Acs Catal* **2022,** *12*, 9307-9324.
25. Martínez, S.; Dydio, P., Multicatalysis enables turning plastic waste into chemical commodities. *Trends in Chemistry* **2023,** *5*, 249-251.
26. Rorrer, J. E.; Ebrahim, A. M.; Questell-Santiago, Y.; Zhu, J.; Troyano-Valls, C.; Asundi, A. S.; Brenner, A. E.; Bare, S. R.; Tassone, C. J.; Beckham, G. T.*, et al.*, Role of Bifunctional Ru/Acid Catalysts in the Selective Hydrocracking of Polyethylene and Polypropylene Waste to Liquid Hydrocarbons. *Acs Catal* **2022,** *12*, 13969-13979.
27. Chen, S.; Tennakoon, A.; You, K.-E.; Paterson, A. L.; Yappert, R.; Alayoglu, S.; Fang, L.; Wu, X.; Zhao, T. Y.; Lapak, M. P.*, et al.*, Ultrasmall amorphous zirconia nanoparticles catalyse polyolefin hydrogenolysis. *Nat. Catal.* **2023,** *6*, 161-173.
28. Zichittella, G.; Ebrahim, A. M.; Zhu, J.; Brenner, A. E.; Drake, G.; Beckham, G. T.; Bare, S. R.; Rorrer, J. E.; Roman-Leshkov, Y., Hydrogenolysis of Polyethylene and Polypropylene into Propane over Cobalt-Based Catalysts. *JACS Au* **2022,** *2*, 2259-2268.
29. Rorrer, J. E.; Beckham, G. T.; Roman-Leshkov, Y., Conversion of Polyolefin Waste to Liquid Alkanes with Ru-Based Catalysts under Mild Conditions. *JACS Au* **2021,** *1*, 8-12.
30. Rorrer, J. E.; Troyano-Valls, C.; Beckham, G. T.; Román-Leshkov, Y., Hydrogenolysis of Polypropylene and Mixed Polyolefin Plastic

Waste over Ru/C to Produce Liquid Alkanes. *ACS Sustain. Chem. Eng.* **2021,** *9*, 11661-66.
31. Du, J.; Zeng, L.; Yan, T.; Wang, C.; Wang, M.; Luo, L.; Wu, W.; Peng, Z.; Li, H.; Zeng, J., Efficient solvent- and hydrogen-free upcycling of high-density polyethylene into separable cyclic hydrocarbons. *Nat. Nanotechnol.* **2023**.
32. Tan, J. Z.; Hullfish, C. W.; Zheng, Y.; Koel, B. E.; Sarazen, M. L., Conversion of polyethylene waste to short chain hydrocarbons under mild temperature and hydrogen pressure with metal-free and metal-loaded MFI zeolites. *Appl. Catal. B* **2023,** *338*.
33. Borkar, S. S.; Helmer, R.; Panicker, S.; Shetty, M., Investigation into the Reaction Pathways and Catalyst Deactivation for Polyethylene Hydrogenolysis over Silica-Supported Cobalt Catalysts. *ACS Sustain. Chem. Eng.* **2023,** *11*, 10142-10157.
34. Hancock, J. N.; Rorrer, J. E., Hydrogen-free catalytic depolymerization of waste polyolefins at mild temperatures. *Appl. Catal. B* **2023,** *338*.
35. Vance, B. C.; Kots, P. A.; Wang, C.; Hinton, Z. R.; Quinn, C. M.; Epps, T. H.; Korley, L. T. J.; Vlachos, D. G., Single pot catalyst strategy to branched products via adhesive isomerization and hydrocracking of polyethylene over platinum tungstated zirconia. *Appl. Catal. B* **2021,** *299*.
36. Vance, B. C.; Kots, P. A.; Wang, C.; Granite, J. E.; Vlachos, D. G., Ni/SiO2 catalysts for polyolefin deconstruction via the divergent hydrogenolysis mechanism. *Appl. Catal. B* **2023,** *322*.
37. Hinton, Z. R.; Kots, P. A.; Soukaseum, M.; Vance, B. C.; Vlachos, D. G.; Epps, T. H.; Korley, L. T. J., Antioxidant-induced transformations of a metal-acid hydrocracking catalyst in the deconstruction of polyethylene waste. *Green Chem.* **2022,** *24*, 7332-7339.
38. Kots, P. A.; Doika, P. A.; Vance, B. C.; Najmi, S.; Vlachos, D. G., Tuning High-Density Polyethylene Hydrocracking through Mordenite Zeolite Crystal Engineering. *ACS Sustain. Chem. Eng.* **2023,** *11*, 9000-9009.
39. Liu, S.; Kots, P. A.; Vance, B. C.; Danielson, A.; Vlachos, D. G., Plastic waste to fuels by hydrocracking at mild conditions. *Sci. Adv.* **2021,** *7*.
40. Kots, P. A.; Liu, S.; Vance, B. C.; Wang, C.; Sheehan, J. D.; Vlachos, D. G., Polypropylene Plastic Waste Conversion to Lubricants over Ru/TiO2 Catalysts. *Acs Catal* **2021,** *11*, 8104-8115.
41. Madras, G.; McCoy, B. J., Numerical and similarity solutions for reversible population balance equations with size-dependent rates. *J. Colloid Interface Sci.* **2002,** *246*, 356-65.
42. McCoy, B. J.; Madras, G., Discrete and continuous models for polymerization and depolymerization. *Chem. Eng. Sci.* **2001,** *56*, 2831-2836.
43. McCoy, B. J.; Madras, G., Analytical solution for a population balance equation with aggregation and fragmentation. *Chem. Eng. Sci.* **2003,** *58*, 3049-3051.
44. Kostoglou, M., Mathematical analysis of polymer degradation with chain-end scission. *Chem. Eng. Sci.* **2000,** *55*, 2507-2513.
45. Guironnet, D.; Peters, B., Tandem Catalysts for Polyethylene Upcycling: A Simple Kinetic Model. *J. Phys. Chem. A.* **2020,** *124*, 3935-3942.
46. Chang, C. F.; Rangarajan, S., Machine Learning and Informatics Based Elucidation of Reaction Pathways for Upcycling Model Polyolefin to Aromatics. *J. Phys. Chem. A* **2023,** *127*, 2958-2966.
47. Soares, J. B. P.; McKenna, T. F. L., A conceptual multilevel approach to polyolefin reaction engineering. *Can. J. Chem. Eng.* **2022,** *100*, 2432-2474.
48. Xie, T.; Wittreich, G. R.; Vlachos, D. G., Multiscale modeling of hydrogenolysis of ethane and propane on Ru(0001): Implications for plastics recycling. *Appl. Catal. B* **2022,** *316*.
49. Yappert, R.; Peters, B., Population balance models for polymer upcycling: signatures of the mechanism in the molecular weight evolution. *J. Mater. Chem. A* **2022,** *10*, 24084-24095.
50. Keil, F., Diffusion and reaction in porous networks. *Catal. Today* **1999,** *53*, 245-258.
51. Keil, F. J., Multiscale modelling in computational heterogeneous catalysis. *Top Curr Chem* **2012,** *307*, 69-107.

52. Norskov, J. K.; Bligaard, T.; Hvolbaek, B.; Abild-Pedersen, F.; Chorkendorff, I.; Christensen, C. H., The nature of the active site in heterogeneous metal catalysis. *Chem. Soc. Rev.* **2008,** *37*, 2163-71.
53. Medford, A. J.; Kunz, M. R.; Ewing, S. M.; Borders, T.; Fushimi, R., Extracting Knowledge from Data through Catalysis Informatics. *Acs Catal* **2018,** *8*, 7403-7429.
54. Medford, A. J.; Vojvodic, A.; Hummelshøj, J. S.; Voss, J.; Abild-Pedersen, F.; Studt, F.; Bligaard, T.; Nilsson, A.; Nørskov, J. K., From the Sabatier principle to a predictive theory of transition-metal heterogeneous catalysis. *J. Catal.* **2015,** *328*, 36-42.
55. Boudart, M., Heterogeneous catalysis by metals. *J. Mol. Catal.* **1985,** *30*, 27-38.
56. Boudart, M., Catalysis by Supported Metals. In *Adv. Catal.*, Eley, D. D.; Pines, H.; Weisz, P. B., Eds. Academic Press: 1969; Vol. 20, pp 153-166.
57. Hinnemann, B.; Nørskov, J. K., Catalysis by Enzymes: The Biological Ammonia Synthesis. *Top. Catal.* **2006,** *37*, 55-70.
58. Meirow, M.; Luijten, E., Coarse-Grained Modeling of Polymer Cleavage within a Porous Catalytic Support. *ACS Macro Lett.* **2023,** *12*, 189-194.
59. Broadbelt, L. J.; Snurr, R. Q., Applications of molecular modeling in heterogeneous catalysis research. *Appl. Catal. A: Gen.* **2000,** *200*, 23-46.
60. Broadbelt, L. J.; Stark, S. M.; Klein, M. T., Computer Generated Pyrolysis Modeling: On-the-Fly Generation of Species, Reactions, and Rates. *Ind. Eng. Chem. Res.* **2002,** *33*, 790-799.
61. Yanez, A. J.; Natarajan, P.; Li, W.; Mabon, R.; Broadbelt, L. J., Coupled Structural and Kinetic Model of Lignin Fast Pyrolysis. *Energy Fuels* **2018,** *32*, 1822-1830.
62. Harmon, R. E.; SriBala, G.; Broadbelt, L. J.; Burnham, A. K., Insight into Polyethylene and Polypropylene Pyrolysis: Global and Mechanistic Models. *Energy Fuels* **2021,** *35*, 6765-6775.
63. Ramkrishna, D., *Population balances : theory and applications to particulate systems in engineering*. Academic Press: San Diego, CA, 2000.
64. Renshaw, E., *Stochastic population processes : analysis, approximations, simulations*. Oxford University Press: Oxford ;, 2011.
65. Payne, C. M.; Knott, B. C.; Mayes, H. B.; Hansson, H.; Himmel, M. E.; Sandgren, M.; Stahlberg, J.; Beckham, G. T., Fungal cellulases. *Chem. Rev.* **2015,** *115*, 1308-448.
66. Irwin, D. C.; Spezio, M.; Walker, L. P.; Wilson, D. B., Activity studies of eight purified cellulases: Specificity, synergism, and binding domain effects. *Biotechnol. Bioeng.* **1993,** *42*, 1002-13.
67. Barr, B. K.; Hsieh, Y. L.; Ganem, B.; Wilson, D. B., Identification of two functionally different classes of exocellulases. *Biochemistry* **1996,** *35*, 586-92.
68. Nidetzky, B.; Steiner, W.; Hayn, M.; Claeyssens, M., Cellulose hydrolysis by the cellulases from Trichoderma reesei: a new model for synergistic interaction. *Biochem J* **1994,** *298 Pt 3*, 705-10.
69. Hosseini, S. A.; Shah, N., Enzymatic hydrolysis of cellulose part II: Population balance modelling of hydrolysis by exoglucanase and universal kinetic model. *Biomass Bioenergy* **2011,** *35*, 3830-3840.
70. Hosseini, S. A.; Shah, N., Modelling enzymatic hydrolysis of cellulose part I: Population balance modelling of hydrolysis by endoglucanase. *Biomass Bioenergy* **2011,** *35*, 3841-3848.
71. Engel, P.; Bonhage, B.; Pernik, D.; Rinaldi, R.; Schmidt, P.; Wulfhorst, H.; Spiess, A. C., Population balance modelling of homogeneous and heterogeneous cellulose hydrolysis. In *Computer Aided Chemical Engineering*, Pistikopoulos, E. N.; Georgiadis, M. C.; Kokossis, A. C., Eds. Elsevier: 2011; Vol. 29, pp 1316-1320.
72. Lebaz, N.; Cockx, A.; Spérandio, M.; Morchain, J., Population balance approach for the modelling of enzymatic hydrolysis of cellulose. *CJCE* **2015,** *93*, 276-284.
73. Wang, J.; Wang, T.-T.; Luo, Z.-H.; Zhou, Y.-N., Simulation of irreversible and reversible degradation kinetics of linear polymers using sectional moment method. *Chem. Eng. Sci.* **2023,** *275*.
74. Wang, J.; Wang, T. T.; Luo, Z. H.; Zhou, Y. N., Analytical and numerical simulations of

depolymerization based on discrete model: A chain - end scission scenario. *AIChE J.* **2022,** *69*.
75. Stickel, J. J.; Griggs, A. J., Mathematical modeling of chain-end scission using continuous distribution kinetics. *Chem. Eng. Sci.* **2012,** *68*, 656-659.
76. Ho, Y. K.; Doshi, P.; Yeoh, H. K.; Ngoh, G. C., Modeling chain-end scission using the Fixed Pivot technique. *Chem. Eng. Sci.* **2014,** *116*, 601-610.
77. Madras, G.; McCoy, B. J., Time evolution to similarity solutions for polymer degradation. *Aiche J* **1998,** *44*, 647-655.
78. Nitzan, A., *Chemical dynamics in condensed phases : relaxation, transfer and reactions in condensed molecular systems*. Oxford University Press: New York, 2006.
79. Coffey, W.; Kalmykov, Y. P., *The Langevin equation : with applications to stochastic problems in physics, chemistry, and electrical engineering*. Fourth edition. ed.; World Scientific Publishing: Hackensack, New Jersey, 2017.
80. McCoy, B. J., A population balance framework for nucleation, growth, and aggregation. *Chem. Eng. Sci.* **2002,** *57*, 2279-2285.
81. Virtanen, P.; Gommers, R.; Oliphant, T. E.; Haberland, M.; Reddy, T.; Cournapeau, D.; Burovski, E.; Peterson, P.; Weckesser, W.; Bright, J*., et al.*, SciPy 1.0: fundamental algorithms for scientific computing in Python. *Nat Methods* **2020,** *17*, 261-272.
82. Ziff, R. M.; McGrady, E. D., The kinetics of cluster fragmentation and depolymerisation. *J. Phys. A Math* **1985,** *18*, 3027-3037.